# The Cell Wall Integrity MAPK pathway controls actin cytoskeleton assembly during fungal somatic cell fusion.

Antonio Serrano, Hamzeh H. Hammadeh, Natalie Schwarz, Ulrike Brandt and André Fleißner[#]

Institut für Genetik, Technische Universität Braunschweig, Spielmannstraße 7, 38106 Braunschweig, Germany

[#]Corresponding author

André Fleißner

Institut für Genetik

Technische Universität Braunschweig

Spielmannstraße 7

38106 Braunschweig

Germany

Tel: +49-531-3915795

FAX: +49-531-3915765

a.fleissner@tu-bs.de

running title:

MAPK regulation of directed growth

key words:

MAPK, cell fusion, directed growth, cell polarization, cell communication, *Neurospora crassa*

## Summary statement

The CWI MAPK MAK-1 pathway controls actin cytoskeleton assembly at the cell tips through activation of the Rho-GTPase RAC-1 exclusively on somatic cell fusion.


## Abstract

Somatic cell fusion is widely studied in the filamentous fungus *Neurospora crassa*. The interaction of genetically identical germlings is mediated by a signaling mechanism in which the cells take turns in signal-sending and receiving. The switch between these physiological states is represented by the alternating membrane recruitment of the SO protein and the MAPK MAK-2. This dialog-like behavior is observed until the cells establish physical contact, when the cell-wall-integrity MAK-1 is recruited to the contact area to control the final steps of the cell fusion process. This work revealed, for the first-time, an additional MAK-1-function during the tropic growth phase. Specific inhibition of MAK-1 during tropic-growth resulted in disassembly of the actin-aster, and mislocalization of SO and MAK-2. Similar defects were observed after the inhibition of the Rho-GTPase RAC-1, suggesting a functional link between them, being MAK-1 upstream of RAC-1. In contrast, after inhibition of MAK-2, the actin-aster stayed intact, however, its subcellular localization became instable within the cell-membrane. Together these observations led to a new working model, in which MAK-1 promotes the formation and stability of the actin-aster, while MAK-2 controls its positionning and cell growth directionality.

## Introduction

Cell-cell fusion (also known as cell fusion) is fundamental for the development of Eukaryotic organisms. It plays an important role in the asexual development of organisms (so-called somatic cell fusion), in which the cells fuse to create organs (e.g. placenta), different cell types (e.g. osteoclasts) or networks (e.g. fungal mycelia) and in the sexual cycle of haploid cells. Both processes are studied in many different model organisms or cell types (e.g. monocytes, myoblasts, yeast etc) and, interestingly, all share very similar and defined stages. These are: 1) the induction of a competence for cell fusion, in which the cells become potential fusion partners by activating specific developmental programs, 2) the comminment of the two fusing cells, when cells actively express signals and cognate receptors to establish a stable communication that induce cell polarization of both partners and, finally, 3) cell fusion, at which the two cells control the correct merging of the plasma membranes and connection of both cytoplasms (Aguilar et al., 2013). In sexual reproduction this step will continue with the fusion of the genomes and the differentiation of a new organism, while in somatic cells new rounds of cell fusion will form, in some cases, a giant syncitia or, like in filamentous fungi, an interconnected cellular network.

In both types of cell fusion, cells need to respond to a chemoattractant (e.g. pheromones in sexual fusion) and either migrate (chemotaxis) or growth (chemotropism) toward the highest gradient. The correct establishment of cell polarization is essential for the chemotropic response. In fungi, the polarized growth of hyphal cells to chemoattractants is mediated through a highly regulated machinery which involves the activation of mitogen-activated protein kinases (MAPKs) and spatial focalization of polarity core

factors, such as formins, or Rho-GTPases (Aguilar et al., 2013; Berepiki et al., 2010; Lichius et al., 2014; Martin and Arkowitz, 2014). The concentration of formin-created actin at the cell tip is also known as a formin-nucleated actin aster (Dudin et al., 2015; Dudin et al., 2017). In fission yeast, formation of the actin aster is controlled by the formin Fus1 and type V myosins. The formin is needed for nucleation of the actin aster, and type V myosins are essential for the release of cell wall hydrolases, which degrade the cell wall between the interacting cells and allow the culmination of the cell fusion process (Dudin et al., 2015). In budding yeast, actin aster and cable assembly are essential for recruitment of the MAPK Fus3p (Qi and Elion, 2005). In addition, Fus3p positively regulates actin cable assembly through phosphorylation of the formin bni1p (Matheos et al., 2004), yielding a regulatory feedback loop that increases the phosphorylation of Fus3p and therefore the response to the pheromone signal. In filamentous fungi, actin is essential for all types of growth (vegetative growth or cell fusion). Disruption of actin during hyphal extension leads to rapid tip swelling, indicating an important function of actin into polarized growth (Berepiki et al., 2010). A highly dynamic actin aster is also observed in *Neurospora crassa* cells undergoing cell fusion, and disruption of actin also arrests the growth of the interacting cells (Berepiki et al., 2011; Berepiki et al., 2010). Actin is, overall, the main component of the polarization during cell fusion although its implications on the process had not been yet elucidated. Two of the main regulators of actin assembly during fungal growth, the Rho-GTPase RAC-1 and CDC-42, had been extensively studied in *N. crassa*, showing an independent and exclusive role of RAC-1 for cell fusion and CDC-42 for vegetative growth (Lichius et al., 2014).

The cell fusion process in *N. crassa* is characterized by the alternating oscillatory recruitment of the MAPK MAK-2 (homolog to Fus3p), and the protein SO, to the opposite tips of the interacting cells. The recruitment of each factors is hypothesized to represent two physiological states on the cells: signal sending and signal receiving, with two very different developmental programs (Fleissner et al., 2009; Goryachev et al., 2012; Serrano et al., 2017). During the cell fusion interaction, the cells switch between the two states, which relies on switching of the recruitment of MAK-2 and SO. After cells establish physical contact, the growth is arrested and cell wall and plasma membrane remodeled to allow the complete fusion and mixing of the cytoplasm. A second MAPK, the cell-wall-integrity (CWI) MAK-1, is only recruited after the cells establish physical contact, and the chemical inhibition of an analog-sensitive variant results in the disruption of the cell merger, suggesting that the kinase activity is essential for the process (Weichert et al., 2016). Interestingly, MAK-1 as well as MAK-2 and SO are essential for the process and the mutation of their respective genes results in the complete absent of cell fusion (Fleissner et al., 2005; Fu et al., 2011; Pandey et al., 2004). This suggests that MAK-1 (besides MAK-2 and SO) is essential for the establishing of a competence state on the cells for cell fusion. However, no conclusive data have shown whether MAK-1 is needed for the communication phase of the cell fusion process, which is featured by the oscillatory recruitment of MAK-2 and SO and the release and sensing of the so-far unknown fusion signal.

In this study, we will address the question on MAK-1 functionality during the communication phase of the cell fusion process and the implications of MAK-2 regulation. We will follow a chemical genetics strategy in order to answer these questions.

## Results

### *MAK-1 kinase-activity inhibition results in disruption of the cell fusion process*

The CWI MAPK MAK-1 plays important functions for the sucessful completion of the cell fusion process. This kinase plays an unknown essential role during the establishment of the cell fusion competence and, in addition, its activity is crucial for the growt arrest of the fusing cells after establishing physical contact (Fu et al., 2011; Weichert et al., 2016). While these data indicate that MAK-1 is required for the onset of the fusion process and after cell-cell contact, it remains unclear if this MAPK also plays a role during the tropic interaction of the fusion partners. Since the deletion of the *mak-1* gene results in the complete disruption of the cell fusion competence (Fu et al., 2011), we decided to turn into the creation of an analog-sensitive version, also known as *Shokat* allele (Bishop et al., 2000), of *mak-1* to manipulate its activity in a spatio-temporal manner. For that purpose, the point mutation that renders the encoded kinase analog-sensitive was integrated at the original gene locus. The gatekeeper amino acid was identified in a previous study (glutamine at position 104) and exchanged by glycine, resulting in the *mak-1*$^{E104G}$ gene which encoded the analog-sensitive kinase (Weichert et al., 2016). The plasmid 738 containing the *mak-1*$^{E104G}$*-hph* construct (details on Mats and method section), was used as a template to amplify the full-length knock-in fragment by PCR (using primers 1304 and 1307), which was transformed into the *N. crassa* strain N1-06 (FGSC 9719) (Fig. S1A). This recipient strain possesses a mutation in the gene *mus52* (*mutagen sensitive 52*), whose gene product is required for DNA repair by nonhomologous end-joining .The mutation results in an increase in the frequency of homologous recombination up to almost 100% (Ninomiya et al., 2004). The resulting

transformants were first tested by PCR by amplifying the *mak-1* locus and the fragment was sequenced to confirm the base pair exchange (E104G; CAG to GGC). The proper integration of the transforming DNA and the absence of additional heterologous integrations were successfully tested by Southern blot of homokaryotic isolates obtained from a sexual cross of the primary transformants with the wild-type strain (Fig. S1A and B). The resulting homokaryotic strain, 849 (similar observations were made in 848, 850 and 851), appeared macroscopically wild type-like, indicating that the mutated kinase is functional in absence of the inhibitor (ATP-analog, 1-NM-PP1) and supplemented with 1% DMSO (solvent of the 1-NM-PP1) as a control (Fig. S1C). In contrast, addition of the inhibitor (40 µM final concentration) to the growth medium resulted in a Δ*mak-1*-like phenotype, whilst the wild-type control strain remained unaffected (Fig. S1C). Microscopically, the presence of the inhibitor drastically reduced the cell fusion rate of the MAK-1$^{E104G}$ strain, proving that it can be inhibited, and allowing us to analyze the functions of MAK-1 at specific stages of the cell fusion process, such as the tropic growth phase (Fig. S1D). Additionally and as previously shown in other publications, neither the solvent DMSO nor the ATP-analog have any effect on wild-type cells, proving its specificity to analog-sensitive variants (Fig. S1C and D).

***Inhibition of MAK-1 during the tropic growth phase results in disruption of MAK-2/SO and actin cytoskeleton***

In order to test the consequences of MAK-1 inhibition during the cell-cell communication steps, multiple strains were created. The most important proteins involved in the cell fusion process are MAK-2 and SO, so we decided to first test the localization of these two after MAK-1 inhibition. The strain carrying the *mak-1::mak-1$^{E104G}$-hph* (849) genotype was

independently crossed with the strains *his-3::Ptef-1-mak-2-gfp* (665) and *his-3::Ptef-1-so-gfp* (714), resulting in strains 865 and 874, respectively. Both strains were tested by PCR for integration of the *mak-1::mak-1*$^{E104G}$*-hph* locus and by fluorescence microscopy for each GFP construct integration. Microscopically, all strains showed comparable MAK-1 inhibition phenotypes at the presence of 1-NM-PP1 (data not shown). When cell-cell communication was observed with the microscope, the addition of DMSO did not affect the normal oscillatory recruitment of MAK-2 (Fig. 1A). However, addition of the kinase inhibitor completely disrupted the cell-cell communication process, and the usual dynamic localization of MAK-2 was interrupted. The kinase disappered from the membrane and no detachment was observed after almost 18 minutes (Fig. 1B). Similarly, addition of DMSO did not affect the usual oscillatory recruitment of SO (Fig. 1C). However, 10 minutes after addition of the kinase inhibitor, SO was accumulated at the membrane in both cell tips at the same time, and the GFP signals were more widely distributed around the cell tips (Fig. 1D). Taken together these data indicate that MAK-1$^{E104G}$ activity is essential for the tropic growth phase and for proper MAK-2 and SO dynamics. As previously described, cell fusion is observed at the early stage of colony establishment between germinated and ungerminated spores, but also later in development between hyphae in the inner part of the fungal colony in a process known as hyphal fusion.

In previous work, we showed that the characteristic MAK-2/SO dynamics also occur during hyphal fusion (Serrano et al., 2018). In order to test whether MAK-1 also plays a role during hyphal fusion, we tested the consequences of MAK-1 inhibition by microscopic analysis of hyphal fusion events. With DMSO, MAK-2 oscillated in a wild-type manner (Fig. S2A). When MAK-1$^{E104G}$ was inhibited, MAK-2 showed a disruption of their dynamics

similar to the findings in germlings (Fig S2B). When looking to SO, DMSO did not affect the usual oscillatory dynamics (Fig. S2C), but addition of the inhibitor completely disrupt the process (Fig. S2D). While MAK-2 completely vanished from the hyphal tip, SO remained as single dots distributed widely around the plasma membrane of both interacting hyphae. These data indicate that the function played by MAK-1 during germling fusion is also conserved in hyphal fusion.

In fungi, proper actin organization is crucial for polarized hyphal extension. In *N. crassa*, Berepiki *et al* adapted a method for indirect actin visualization: the actin-reporter life-act linked to GFP (Berepiki et al., 2010). Lifeact is a small peptide (17 amino-acid), which represents the N-terminus of the actin-binding protein Abp140 from *S. cerevisiae* (Riedl et al., 2008). In non-interacting cells of *N. crassa* expressing this reporter, actin is mainly found at the tips of growing germ tubes, in the form of actin patches localized around the cell tips and actin cables. During cell fusion, disruption of actin assembly results in failure of polarized, directed growth of the fusion tips, while microtubules are dispensable for this process (Roca et al., 2010). Additionally, in *S. pombe* mating fusion, actin also accumulates at the Shmoo of the interacting cells in a structure termed actin fusion aster complex. This accumulation has been shown to mediate the release of cell wall degrading enzymes involved in fusion pore formation (Dudin et al., 2015). All these data indicate that actin is essential for tropic growth and cell fusion, but its regulation remains mostly unknown. In order to test whether MAK-1 influences actin assembly and dynamics, we created a strain carrying the *mak-1::mak-1*$^{E104G}$*-hph* construct together with the *his-3::Ptef-1-lifeact-gfp* expression cassette, by crossing of strains 849 and 754, respectively, resulting in strain 869. This isolate behaved as wild type in the presence of DMSO, and

typical actin cables were present at the cell tips during the communication phase and during cell merger comparable to wild-type cells. To our surprise, actin dynamics showed a comparable oscillatory and alternating accumulation at the cell tips of the interacting cells as MAK-2 and SO (Fig. 1E). When MAK-1$^{E104G}$ was inhibited by addition of the kinase inhibitor, actin accumulation was clearly affected. Interestingly, the accumulation of actin cables from the tips disappeared. In addition, actin patches were not focused anymore around the cell tips, but localized in a wider distribution around the cell membrane of the entire cell body (Fig. 1F). As expected, actin oscillation was also observed in hyphal fusion (Fig. S2E). Inhibition of MAK-1$^{E104G}$ also disrupted actin accumulation at the hyphal tips as observed in germling fusion (Fig. S2F).

These data suggest for the first time that MAK-1 might be involved in the regulation of the actin cytoskeleton during the cell fusion process. An alternative explanation might be that the actin misregulation represents an indirect effect of the disruption of the cell fusion process in the cells. This will be addressed in the following sections.

***Actin accumulation at the cell tips oscillates out-of-phase of SO/MAK-2 usual dynamics***

Surprisingly, the observation of actin localization in the MAK-1 inhibitable strain in the presence of DMSO suggested that accumulation of actin occurs at the cell tips of the interacting cells and that this accumulation oscillates in an antiphase manner. To further decipher whether it was a specific effect of this strain, we decided to observe the localization of actin on wild-type cells. By using the strain 754 (Berepiki et al., 2010) in which the construct *lifeact-gfp* is transformed into the *his-3* locus in the wild-type

background, we made similar observations on actin accumulation at the cell tips and its oscillation in an antiphase manner (Fig. 2A). Based on these data, we hypothesized that actin accumulation is likely observed together with SO, since the presence of SO at the cell tips is associated with a signal sending state of the fusing cell (Fleißner and Serrano, 2016; Goryachev et al., 2012). We therefore created a strain (H99) expressing both genes in the *his-3* locus, lifeact-GFP and SO-mCherry, to allow observation of actin and SO within the same cell. When interacting cell pairs were observed, a dynamic interferes co-localization was found, in which SO was recruited to the membrane at the tip of the first pair while actin was recruited in the second interacting cell. After a few minutes, both proteins co-localize at the tip of the first partner. Lastly, actin disassembled form the membrane of the upper cell and was recruited in the lower cell, while SO stayed at the tip of the upper cell. (Fig. 2B). This indicates that actin polymerization at the cell tips is out-of-phase of the usual dynamics of MAK-2/SO. To test whether actin oscillates during vegetative growth, germinated spores of strain 754 (expressing lifeact-gfp in the WT background) were observed under the fluorescence microscope. Actin was localized to the cell tips of growing cells as previously described (Berepiki et al., 2010) and no oscillation was observed (Fig 2C), indicating that oscillatory accumulation of actin is exclusive of the cell fusion growth.

***Inhibition of MAK-2 results in disruption of the usual MAK-2/SO and actin localization during cell fusion***

Based on the previous results, we hypothesized that MAK-1 may be directly involved in actin polimerization or that actin misregulation may be an indirect effect of the disruption of the cell fusion process caused by MAK-1 inhibition. To test this hypothesis, we decided

to follow a similar strategy by creating an analog-sensitive version of MAK-2 to decipher SO and actin dynamics during the tropic growth phase.

Similar to the design of the *mak-1*$^{E104G}$*-hph* construct, a *mak-2*$^{Q100A}$*-hph* gene knock-in cassette was created and integrated at the original gene locus of strain N1-06 (Δ*mus-52*). However, this construct proved to be not functional and the respective transformants exhibited a Δ*mak-2*-like phenotype (data not shown). In previous studies, we found that the Δ*mak-2* phenotype of the knock-out mutant was only fully complemented when the analog-sensitive version was overexpressed by using strong constitutive promoters such as *Pccg-1* or *Ptef-1* (Fleissner et al., 2009; Serrano et al., 2018). We therefore decided to replace the promotor at the original gene locus by the P*tef-1* sequence. The linear *Ptef-1-mak-2*$^{Q100A}$*-hph* knock-in cassette (details on Mats and Methods section) amplified from the plasmid 846 with primers 1487 and 1488 was transformed into N1-05 (Δ*mus-52* like N1-06, but different mating type) resulting in strain 882 (*Pmak-2-mak-2::Ptef-1-mak-2*$^{Q100A}$*-hph*) (Fig. S3A). The primary transformants were tested by PCR of the *mak-2* locus and sequencing of the resulting fragment. In order to obtain a homokaryotic strain, a sexual cross was performed between wild type *mat a* (N1-02) and one of the primary transformants, 882 (*mat A*). Four of the resulting progenies were tested by Southern blot analysis for single integration of our construct. All four isolates showed clear bands corresponding to the *Ptef-1-mak-2*$^{Q100A}$ radioactive-labelled fragment, while it was absent in the recipient strain (N1-05) (Fig. S3A and B). The generated strains showed a macroscopic phenotype like wild type in the absent of the kinase inhibitor (plus DMSO) and a Δ*mak-2*-like phenotype when it was present (Fig. S3C). Microscopically, cell fusion rates were not fully comparable to the wild-type strain in the present of DMSO, but cell

fusion was still observed. In contrast, cell fusion rate was comparable to Δ*mak-2* when the kinase inhibitor was added (Fig. S3D). These data indicate that the strain is functional for cell fusion in the absent of the kinase inhibitor and allow us to analyze the cell dynamics when MAK-2$^{Q100A}$ is inhibited in a spatio-temporal manner.

To test the effect of MAK-2$^{Q100A}$ inhibition on the localization of SO and actin, we crossed the strain *Pmak-2-mak-2::Ptef-1-mak-2$^{Q100A}$-hph* (899) independently with *his-3::Ptef-1-so-gfp* (714) and *his-3::Ptef-1-lifeact-gfp* (754), generating the strains *his-3::Ptef-1-so-gfp; Pmak-2-mak-2::Ptef-1-mak-2$^{Q100A}$-hph* (912) and *his-3::Ptef-1-lifeact-gfp; Pmak-2-mak-2::Ptef-1-mak-2$^{Q100A}$-hph* (915), respectively. When cell fusion was observed with DMSO, the dynamic localization of SO was wild-type-like and no significant differences to the reference strain were observed (Fig. 3A). When the kinase inhibitor was added, the oscillation rapidly ceased (after around 4 minutes) and, in 10/15 observations, the localization of SO remained widely distributed around the cell membrane (Fig. S4A). Interestingly, in 5/15 observations, the localization of SO switched to another area of the cell, suggesting that the complex formed at the cell tips may travel together around the cell-membrane after MAK-2 inhibition (Fig. 3B). Regarding actin localization, fusing cell pairs were observed under the microscope with DMSO, showing the already described oscillatory accumulation of actin to the cell tips (Fig. 3C). In the presence of the kinase inhibitor, the actin localization switched to a different spot within the cell, in some of the cases (10/20) travelling to the opposite cell tip, in a similar manner than SO (Fig. 3B). After 10 minutes, actin was still accumulated at the new spots although the tropic interaction and directed growth were already terminated (Fig. 3D). We also observed in some cases (10/20) than actin switched to a different position, but remaining close to the

cell tip (Fig. S4B). These data clearly indicate that MAK-2 inhibition leads to a slightly different disruption of the actin localization, suggesting that MAK-1 and MAK-2 play different roles on the cytoskeleton organization during cell fusion and excluding the hypothesis of the indirect effect on actin cytoskeleton due to the cell fusion disruption.

***The actin cytoskeleton is essential for the dynamic localization of MAK-2 and SO***

MAK-1$^{E104G}$ inhibition disrupts the proper MAK-2/SO membrane recruitment. At the same time, actin accumulation at the cell tips is also disturbed. Actin cables serve as tracks for the transport of multiple cargoes, including potential secretory vesicles, which might be involved in the cell fusion process (Berepiki et al., 2011; Dudin et al., 2015). Our data support two alternative hypotheses: either MAK-1 activity is directly involved in both MAK-2/SO recruitment and actin organization, or it is only involved in actin organization, but actin disruption results in a disturbed MAK-2/SO localization.

In yeast, Fus3p recruitment is mainly mediated through actin cables organized at the Shmoo of the mating cells (Qi and Elion, 2005). In order to test whether actin is needed for proper MAK-2/SO recruitment, we employed the actin-disrupting drug latrunculin A. This toxin originating from the Red Sea sponge *Latrunculia magnifica* binds to actin monomers, thereby preventing the formation of F-actin (Coué et al., 1987). In *N. crassa*, it has been used to demonstrate that actin is essential during the cell fusion process, but without testing the effect on MAK-2/SO dynamics (Berepiki et al., 2010).

In a pretest we determined that a concentration of 10 μM resulted in the disassociation of F-actin in germinating spores within 6 minutes (Fig. S4C). When MAK-2 localization was tested, we observed that actin disruption due to latrunculin A resulted in the dissasimble

of MAK-2 after 8 minutes, and no further MAK-2 membrane recruitment was observed in the cells (Fig. 4A). Similarly, the dynamic localization and membrane recruitment of SO were also affected by actin inhibition (Fig. 4B), suggesting that the proper polymerization of actin at the cell tips is essential for membrane recruitment of MAK-2 and SO. To further understand the implications of MAK-1/MAK-2 in this process, we decided to investigate the roles of the upstream regulators of actin polymerization, the Rho-GTPases.

Rho GTPases are signaling G proteins conserved in all eukaryotic organisms that regulate intracellular actin dynamics. These proteins cycle between an active (GTP-bound) and an inactive (GDP-bound) conformation (Martin and Arkowitz, 2014). Upon activation, the Rho GTPases translocate from the cytosol to the plasma membrane, where they interact with actin polymerization proteins, such as formins, that regulates the formation of actin cables (Berepiki et al., 2011).

In *N. crassa*, the Rho-type GTPase RAC-1 is essential for cell fusion, while the Rho-type GTPase CDC-42 plays a role in germination and normal polarized germ tube growth. Both proteins localize to the tips of growing cells (Lichius et al., 2014). To differentiate the functions of both Rho-type GTPases, the specific RAC-1 inhibitor NSC3766 was employed in an earlier study. The drug only affects RAC-1 but not CDC42 and had already been used and proved functional in *N. crassa* (Lichius et al., 2014). In our experiments, we tested if the specific inhibition (with NSC3766) of RAC-1 would affect the dynamics of actin and the recruitment of MAK-2, SO and actin assembly. In interacting cell pairs expressing MAK-2-GFP, the protein was recruited to the membrane in a wild-type manner before addition of NSC3766. The addition of NSC23766 at a concentration of 100 μM resulted in defects in the recruitment of MAK-2 after 12 minutes. MAK-2 fully disappeared

from the membranes of both cells and the interaction ended (Fig. 4C). When SO dynamics were tested, the usual membrane accumulation at the cell tips was observed. Like the previous experiment, defects in the localization of SO were observed 12 minutes after the addition of the RAC-1-inhibitor. However, in contrast to MAK-2, SO remained widely distributed at the membranes of both cells although the interaction had ended (Fig. 4D). This mislocalization of SO was comparable to the one observed after MAK-1 inhibition (actin patches distributed all around the cell membrane), suggesting that both proteins (MAK-1 & RAC-1) may play functions within the same pathway.

Actin localization was also tested in the presence of the RAC-1 inhibitor. When the inhibitor was added, the number of actin cables declined and actin patches were distributed more widely around the plasma membrane. After 12 minutes, actin cables fully disappeared and directed cell growth halted (Fig. S4D). All these data indicate that the proper polymerization of actin at the cell tips of the interacting cells, through activation of the Rho GTPase RAC-1, is essential for the dynamic localization of MAK-2 and SO.

***MAK-1 activity is essential for activation of RAC-1 while MAK-2 activity is important for its positioning***

All previous experiments suggest a potential connection between MAK-1 activity and RAC-1 activity. Both proteins are essential for actin assembly during cell fusion, and similar defects are observed when each one is inhibited. In contrast, MAK-2 inhibition disrupts the cell communication process although the actin aster becomes unstable within the cell. Together, these data support two potential hypotheses: MAK-1 and RAC-1 function in the same pathway (either upstream/downstream), which controls actin

polymerization, or RAC-1 and MAK-1 regulate, independently, a common target that is essential for actin assembly (e.g. the formin BNI-1).

To test these hypotheses, we decided to analyze active RAC-1 dynamics after MAK-1 and MAK-2 inhibition through visualization by the Cdc42-Rac-interacting-binding (CRIB) reporter (see below). If our first potential hypothesis is correct, the outcome of the experiment will show that MAK-1 inhibition results in inactivation of RAC-1 and therefore membrane detachment of the reporter since Rho-GTPases are membrane-recruited only when are activated (Araujo-Palomares et al., 2011; Corvest et al., 2013). If the second hypothesis is correct, we should observe that MAK-1 inhibition does not have any effect on RAC-1 activation, and therefore the reporter should remain activated and attached at the plasma membrane, indicating that MAK-1 and RAC-1 control independently the same factor, that is involved in actin polymerization during cell fusion.

The use of CRIB reporters in *N. crassa* was established by Lichius and colleagues. They created a GFP-labelled reporter that binds as a GEF protein to activated Rho-GTPases without disrupting their function, thereby allowing to localize both activated RAC-1 and CDC-42 at the same time (Lichius et al., 2014). The use of the RAC-1 inhibitor allowed them to distinguish the functions of both proteins. The CLA-4 CRIB reporter strain (*Pccg1::crib^cla-4-gfp::bar*$^{+}$, 927) was crossed with the MAK-1$^{E104G}$ strain (849), resulting in strain 943 (*mak-1::mak-1*$^{E104G}$*-hph; Pal1-crib*$^{cla-4}$*-bar*). As a control we first tested the already reported effects of RAC-1 inhibition on the CRIB reporter. As previously reported, the addition of the RAC-1-specific inhibitor NSC23766 to interacting cells resulted in vanishing of the reporter from the apical tip and cell growth arrest (Fig. S5A). The complete disappearance of the reporter from the tips of the interacting cells indicates that

only RAC-1 and not CDC-42 is present at the growth cone of the fusing cells, since CDC-42 is not affected by the RAC-1 inhibitor.

In our control, we observed as already shown that the CRIB reporter was present permanently in both cell tips during fusion (Fig. 5A) (Lichius et al., 2014). When in the next step, MAK-1 was inhibited, the CRIB reporter disappeared from the plasma membrane and cell growth was arrested (Fig. 5B). Interestingly, both RAC-1 and MAK-1 inhibition showed a similar effect on the CRIB reporters, suggesting that likely the inhibition of MAK-1 specifically affect RAC-1 activity, therefore disrupting the actin assembly, membrane recruitment of MAK-2 and SO and the general fusion process.

Consistent with our hypothesis, MAK-2 inhibition should not affect the activity of RAC-1, but rather its localization, as we have observed with the actin in previous experiments. To test this, the CRIB reporter strain (927) was crossed with MAK-2$^{Q100A}$ (899), resulting in strain 949 (*Pmak-2-mak-2::Ptef-1-mak-2$^{Q100A}$-hph;Pal1-crib$^{cla-4}$-bar*). Like previously, the localization of the CRIB reporter stayed permanently at both cell tips during the whole tropic growth phase in our control (Fig. 5C). When MAK-2 was inhibited, the CRIB reporter remained recruited to the plasma membrane and its localization appeared to be widely distributed around the cell tip (Fig. 5D). These data suggest that MAK-2 might be controlling the localization, and therefore growth directionality, of the Rho-GTPase RAC-1.

However, we already mentioned that the CRIB reporter allows the localization of the activated forms of RAC-1 and CDC-42 at the same time (Lichius et al., 2014). To decipher if RAC-1, and not CDC-42, is switching its position after MAK-2 inhibition, we used the

RAC-1 inhibitor after inhibition of MAK-2. Like the previous experiments, fusing cells were observed under the microscope and the kinase inhibitor was added. After observing, again, the switching in the position of the CRIB reporter provoked by the inhibition of MAK-2, the RAC-1 inhibitor was added. Interestingly, the CRIB reporter fully disappeared from the plasma membrane, indicating that MAK-2 inhibition of fusing cells affects exclusively the position of RAC-1 at the plasma membrane (Fig. 5E). These data indicate that MAK-2 inhibition in tropically growing cells specifically affects the localization of RAC-1 (that stays active), which remains recruited to the plasma membrane but loses growth directionality towards the cell fusion partner and changes its position to another area in the cell.

Together, all these data support a model in which inhibition of MAK-1 specifically affects RAC-1 membrane recruitment, which then results in disassembly of the actin focus organized by the Rho-GTPase and arrest growth of the interacting cells.

***MAK-1 exclusively controls actin polymerization during cell fusion***

We have shown that MAK-1 activity is essential for the correct polimerization of actin at the cell tips of the interacting cells and it raises the question whether MAK-1 functions are specific for directed growth or if they are also involved in general polar growth. In order to test this, we decided to observe the effect of the  kinase inhibitor and the RAC-1 inhibitor (as a negative control) independently in non-interacting cells. Under the microscope, we quantified the length of the germ tube before and after incubation of either the kinase inhibitor, the RAC-1 inhibitor or DMSO. To ensure that only non-interacting cells were tested, only germlings with a distance of more than 30 µm to the nearest cell were analyzed. As a result, no significant differences were observed between the DMSO, the

447 kinase inhibitor or the RAC-1 inhibitor, supporting the idea that MAK-1 exclusively
448 regulates actin polimerization and therefore tropic growth during cell fusion (Fig. 6A).
449 Additionally, we also tested whether MAK-2 had any effect on growth rate by performing
450 the same experiment and obtaining similar results (Fig. 6A). Furthemore, we also tested
451 the localization of the CRIB reporter and actin before and after addition of DMSO, the
452 kinase inhibitor or the RAC-1 inhibitor. Observations were made as previously described
453 but using a fluorescence microscope to record the localization of the CRIB reporter or
454 actin. As expected, no consistent differences were observed in the localization of the
455 CRIB reporter when the cells were incubated with DMSO or the kinase inhibitor (Fig. 6B)
456 and with $H_2O$ (solvent of the RAC-1 inhibitor) or the RAC-1 inhibitor (Fig. 6C) in the MAK-
457 1-inhibitable strains. Similarly, no differences were found in the localization of actin when
458 cells were treated with DMSO or the kinase inhibitor (Fig. 6D), or with $H_2O$ or the RAC-1
459 inhibitor (Fig. 6E) in the MAK-2-inhibitable strains. In order to confirm this finding from the
460 chemical genetics approach, we also studied the actin organization in the *mak-1* knock-
461 out mutant. The knock-out strain was obtained from the *N. crassa* gene knock-out
462 collection (NCU09482). As previously reported, the mutant showed a cell fusion-deficient
463 phenotype (Fu et al., 2011). In order to obtain an actin-labelled Δ*mak-1* strain, a sexual
464 cross was set up between the strains Δ*mak-1* and 754 (*his-3::Ptef-1-lifeact-gfp*), resulting
465 in strain 891 (*mak-1::hph;his-3::Ptef-1-lifeact-gfp*). Spores of this isolate were incubated
466 in MM for 2 hours and actin organization was studied by fluorescence microscopy. In the
467 wild-type cells, actin is organized at the growing cell tips and actin cables are expanding
468 from the growing tip (Berepiki et al., 2011). In the Δ*mak-1* mutant cells, germ tube

elongation and actin assembly at the growing cell tips was comparable to wild type (Fig. S5B).

Together, all these data indicate that MAK-1 exclusively function as a actin polymerization regulator during the cell fusion process and is not involved in actin polimerization during general vegetative growth. In other words, MAK-1 is not involved within the same actin-regulatory pathway than CDC-42.

***MAK-1 functions upstream of RAC-1***

As we have already shown, MAK-1 is essential during the communication phase, when MAK-2 and SO are recruited to the cell tips in an oscillatory manner. Additionally, MAK-1 is also important for the growth arrest phase, in which the tropic growth is arrested and cell wall is remodeled to allow the completition of the fusion process. When an analog-sensitive version of MAK-1 is partially inhibited, the growth arrest and cell merger is disrupted and fusing cells exhibit an unique phenotype of corkscrew-like structures (also known a twisting germ tubes) (Weichert et al., 2016). To additionally test whether MAK-1 and RAC-1 are within the same pathway, we decided to analyze the formation of the twisting germ tubes phenotype after partial inhibition of RAC-1 in wild-type cells, as indicated in the previous study (Weichert et al., 2016). Interestingly, the partial inhibition of RAC-1 induced the formation of twisting germ tubes, again indicating that both proteins function in the same pathway. Three different concentrations were tested (100, 50 and 25 µM), albeit only 25 µM allowed the induction of cell fusion events (Fig. 7A). Interestingly, a large number of cells exhibit defects in polar growth, which may be related to the effect of RAC-1 inhibition. To further investigate this, we decided to quantify the

percentage of cells that shows tropic defects (observed as growth-forming circles). First, we quantify the number of cells that underwent this growth after RAC-1 inhibition in a medium with $Ca^{2+}$, and about 12.5% of the cells exhitied this growth (compared to the water control). To show whether this defect may be caused by inhibition of the general germ tube elongation machinery (not related to cell fusion growth), we performed similar quantifications on wild-type cells placed on media without $Ca^{2+}$ (its absent inhibits the induction of cell fusion) and on a cell fusion mutant, such as Δ*so.* We observed that either in absent of $Ca^{2+}$ or in the cell fusion mutant, the polarity defects were not observed (Fig 7B), suggesting that this phenotype may be caused by partial inhibition of RAC-1 only when cells are undergoing cell fusion.

Although MAK-1 and RAC-1 functions within the same actin-regulatory pathway during cell fusion, there are not strong evidences on which is upstream/downstream. Interestingly, both proteins are localized at the cell tips during the cell growth arrest phase. We therefore decided to test how localization of MAK-1 and RAC-1 was affected after inhibition of RAC-1 or MAK-1, respectively. Cells that just established contact were observed in the microscope and either RAC-1 or the kinase inhibitor added to visualize the effect on the subcellular localization of MAK-1/RAC-1. When RAC-1 was under observation, its localization stayed at the contact area of the fusing cells that just made contact and the addition of DMSO did not have any effect on its localization (Fig. 8A). However, the full inhibition of MAK-1 in fusing cells induced a rapid mislocalization of RAC-1, that completely dissappears from the plasma membrane while cells presumibely stop their cellular interaction (Fig. 8B). Addition of water (solvent of RAC-1 inhibitor) did not affect the cell fusion event and MAK-1 localization during the last steps of the cell

fusion (Fig. 8C). Interestingly, addition of the RAC-1 inhibitor in interacting cells as well did not have any significant effect on the localization of MAK-1, that stayed at the contact area, although cells likely stop their interaction (Fig. 8C).

These data clearly indicate that both MAK-1 and RAC-1 play a role within the same actin-regulatory pathway, showing for the first-time that the MAPK MAK-1 controls, and therefore is upstream, activation and membrane-recruitment of RAC-1 during the cell fusion process.

## Discussion

The correct actin-cytoskeleton assembly is essential for the somatic cell fusion in *N. crassa*, which provides on outstanding model for studying actin-dynamics and its regulation. In this study, we show for the first time the molecular insight regulation of the CWI MAPK MAK-1 on actin-assembly, that happens through the activation of the downstream Rho-GTPase RAC-1, to control actin assembly during the communication phase and cell merger. In addition, we described a function of the MAPK MAK-2 on actin reorganization by controlling RAC-1 positioning likely to the higher gradient intensity of the unknown fusion signal generated by the opposite fusing cell.

### MAK-1 plays different roles in CWI regulation and cell fusion

The central and well-described role of the CWI-signaling pathway is to detect and respond to cell wall stresses that arise in the vegetative life cycle of fungi. In yeast, activation of this pathway is well understood and has been reviewed several times (Correia et al., 2010; de Nobel et al., 2000; Levin, 2011).

535 In filamentous fungi, activation of the pathway is mediated by a group of sensor proteins
536 named as WSC (cell wall integrity and stress-response component). These glycosylated
537 transmembrane proteins sense morphological changes induced by cell growth or cell wall
538 stresses. The signal is transduced to the MAPK cascade by the small Rho-GTPase RhoA
539 and the protein kinase C (PkcA). This activation yields a fully phosphorylated MpkA MAPK
540 (homolog to MAK-1) that further activates transcriptional factors mediating the appropriate
541 cellular responses (Yoshimi et al., 2016). In *N. crassa*, WSC-1 and its homolog WSC-2
542 activate the cell wall integrity MAK-1 MAPK pathway when the cell wall is stressed.
543 Deletion of both genes (*wsc-1* and *wsc-2*) results in strong morphological defects during
544 vegetative growth and colony formation (Maddi et al., 2012), which is very similar to the
545 observations made in the different mutants of the CWI MAPK MAK-1 pathway (Maerz et
546 al., 2008; Park et al., 2008; Vogt and Seiler, 2008). In addition to these defects in cell wall
547 stress response, mutation of every component of the MAK-1 MAPK module also results
548 in a cell fusion-defective phenotype (Fu et al., 2011). However, while the kinases are
549 essential to undergo cell fusion, WSC-1 and WSC-2 are dispensable for this process,
550 indicating that for the cell fusion process MAK-1 is activated independently of the CWI
551 pathway (Maddi et al., 2012).

552 Another upstream activator of MAK-1 is the HAM-7 protein. HAM-7 is a GPI-anchored
553 cell wall protein that is required for activation of MAK-1 (Maddi et al., 2012). Together with
554 HAM-7, the proteins HAM-6 and HAM-8 are hypothesized to work together in a complex
555 as a sensor of signals to trigger MAK-1 phosphorylation (Fu et al., 2014). Mutation of
556 either *ham-6*, *ham-7* or *ham-8* results in a cell fusion defective phenotype, therefore
557 suggesting that its function might be related to activation of MAK-1 for cell fusion

purposes. All these clearly suggest and support the idea that MAK-1 is activated by two different set of sensors: the WSC complex that mediates the signals related to the cell wall stresses and the HAM-6/HAM-7/HAM-8 sensor which is more associated to the signals coming from the cell fusion process. In future studies, it will be of interest to investigate the functions of these three proteins by controlling its expression with inducible promoters and observe the defects induced in the cell fusion (e.g. twisting germ tubes).

**MAK-1 functions in all of the three main cell fusion steps: competence, signaling and growth arrest**

As shown before, cell fusion comprises several independent steps: first the cells need to acquire a cell fusion competence. Second, the cells recognize the presence of other cells and start the tropic growth including the membrane recruitment of MAK-2 and SO. Third, the cells establish physical contact, their growth is arrested and the cell wall is remodeled in order to allow the subsequent fusion of the plasma membranes of both interacting cells. In previous studies, MAK-1 had been shown to play potential functions during competence and growth arrest. It is known that the mutation of *mak-1* results in a cell fusion defective phenotype, in which cells fail to initiate interactions (Fu et al., 2011), indicating that the cells need MAK-1 in order to start the cell fusion process. This also suggests that MAK-1 plays a role in the activation of different factors that allow the acquisition of the competence state by the cell.

One of these potential factors might be the Rho-GTPase RAC-1. As it has been previously shown, mutation of *rac-1* also leads to a fusion defective phenotype and its inhibition results in the loss of the ability of the cells to undergo cell fusion (Araujo-Palomares et al.,

2011; Lichius et al., 2014). Our experiments revealed that inhibition of MAK-1 results in inactivation of RAC-1 and the failure of the cells to initiate interactions. We therefore hypothesize that an active version of RAC-1 is needed to establish the cell fusion competence in the cell and this activation is probably mediated by MAK-1. One way to test if a mutant is blocked in the cell fusion competence state is to analyze its ability to form CATs. For example, the mutation of *so* results in spores that are fusion defective, but are still able to form CATs in the presence of wild-type cells, suggesting that the cells are still fusion competent but unable to undergo the subsequent communication process and directed growth (Fleissner et al., 2005). To analyze whether RAC-1 is also affected in this state, a mix of Δ*rac-1* and wild-type spores should be analyzed by light microscopy to observe whether CATs are formed. RAC-1 inhibition studies could also be performed, by mixing of inhibited and uninhibited wild-type cells. These experiments would elucidate whether RAC-1 is essential for cell fusion competence and would also help to solve the implications of MAK-1 to this process.

As previously mentioned, MAK-1 also plays a role after the cells have established physical contact, specifically in growth arrest and fusion pore formation. During the communication phase, when MAK-2 and SO are dynamically recruited to the tips of the interacting cells, MAK-1 remains cytoplasmic. The protein is only localized to the contact area of the cells after establishment of cell-cell contact, once cell growth is arrested and fusion pore is being formed (Weichert et al., 2016). Interestingly, partial inhibition of MAK-1 which still allows fusion competence and the tropic cell-cell interaction, results in a unique phenotype, in which the interaction partners fail to arrest growth after cell-cell contact and twist around each other.

Together these observations suggest a role of MAK-1 in the recognition of cell-cell contact and subsequent growth arrest. A similar failure in cell growth arrest is observed in the Δ*erg-2* strain. The *erg-2* (*ergosterol-2*) gene encodes a sterol reductase, which mediates the last step of the ergosterol biosynthesis in *N. crassa*. In this mutant, MAK-1 is not recruited to the contact area and the twisting germ tubes phenotype is also observed (Weichert et al., 2016). Interestingly, a potential connection between MAK-1 partial inhibition and membrane sterol composition is the Rho GTPase RAC-1. The membrane recruitment of Rho GTPases is dependent of the proper accumulation and synthesis of sterol-rich membrane (SRM) domains which are defined by the sterol composition of the membrane (Makushok et al., 2016). This suggest that the defects reported in the sterol-biosynthesis mutant (Δ*erg-2*) (Weichert et al., 2016), could be caused by defects in the composition and formation of the SRM domains, which may partially affect the proper localization and likely activation of the Rho-GTPase RAC-1. It will also explain why partial inhibition of MAK-1, which we can assume also cause partial inhibition of RAC-1, produced a similar phenotype. In future studies, it will be of great interest to observe whether the localization of activated RAC-1 (CRIB reporter) is affected in the Δ*erg-2* strain.

**MAK-1 is essential for maintenance of the directed growth machinery while MAK-2 controls the direction of the growth**

As discussed above, MAK-1 possesses functions during two of the cell communication steps: fusion competence and growth arrest after cell-cell contact. In this study we show for the first time that, in addition, MAK-1 also plays a role during the phase of cell-cell signaling and directed growth.

Specific inhibition of MAK-1 during this stage of the fusion process revealed that the kinase is essential for the maintenance of an actin cluster formed by actin filaments at the growing cell tips. This function seems to be again linked to the small Rho-type GTPase RAC-1, whose inhibition results in a comparable disintegration of the actin aster, suggesting that both factors function in the same pathway. Localization of activated RAC-1 (visualized by the CRIB reporter) at the cell tip also required MAK-1 activity, suggesting that MAK-1 functions upstream of RAC-1, meanwhile inhibition of RAC-1 does not disrupt MAK-1 localization at the contact area of the fusing cells.

Our testing of the specific function of the Fus3p homolog MAK-2 in *N. crassa* cell fusion revealed that the kinase is essential for the correct positioning of the actin cluster within the cell. Consistent with our findings that MAK-1 and RAC-1 function in the same pathway organizing the structure of this aster (see above) also the position of RAC-1 becomes instable after MAK-2 inhibition. Future experiments should co-localize actin, the only known formin in *N.* crassa, BNI-1, and RAC-1 after MAK-2 inhibition. If our hypothesis is correct, all factors should co-localize in the same instable fashion after MAK-2 inhibition (meaning they should all move around together in the inhibited cell). A major unanswered question is how MAK-2 is positioning the actin cluster at the proper position in the cell, thereby controlling growth directionality. We hypothesize that MAK-2 is directly involved in the translocation of the cell-cell communication signal and is therefore marking the position of highest signal intensity. Unfortunately, so far this signal and its cognate receptor remain unknown. Common candidates, such as G-Protein coupled receptors or histidine kinases could be excluded (Fleißner and Serrano, 2016). Future experiments

should therefore aim to identify the signal, the upstream activators of MAK-2, and MAK-2 targets involved in positioning the actin cluster.

All together, the results obtained in this study support a model in which MAK-1 functions as a key activator of actin reorganization during cell fusion. This activation occurs through the Rho-GTPase RAC-1 which is the main organizer and also activator likely of the only known formin in *N. crassa*, BNI-1. This actin reorganization is essential for the growth of the fusing cells and therefore for somatic cell fusion. In contrast, MAK-2 plays the role of positioning the actin cluster around the tip in order to respond and grow towards the highest produced gradient of fusion signals. This way the cells are able to recognize the presence of fusing partners in their surroundings and grow towards each other in order to complete the fusion event.

## Material and methods

*N. crassa strains and media*

The strains generated and used in this study are listed in the supplementary information (Table S1). Strains were generally grown in Vogel's Minimal Medium (VMM) (Vogel, 1956) supplemented with 2% sucrose as the carbon source and with 1.5% agar for solid media. Generally, all strains were incubated in solid VMM (supplemented with histidine 0.5 mg/ml when needed) for 3-4 days in dark at 30ºC and an additional day with natural light at room temperature. Homokariotic strains were purified by either single spore isolation (SSPi) or by crossing with the wild-type strain. For selection during SSPi, VMM with hygromycin was employed. Crosses were performed on Westergaard's medium as described earlier (Westergaard and Mitchell, 1947). The ascospores obtained from the

crosses were germinated in VMM with hygromycin and confirmed by polymerase chain reaction (PCR).

*Plasmid construction*

The primers used for the generation of the plasmids are listed in table S2. In order to construct the *mak-1*$^{E104G}$ (analog-sensitive) knock-in cassette, a fragment containing a 5´ upstream region together with the *mak-1* open reading frame was PCR-amplified using the primers 1304 and 1305 and using the previously generated *mak-1*$^{E104G}$*-gfp* plasmid as a template (Weichert et al., 2016). By yeast recombinational cloning, the resulting fragment was fused to the hygromycin resistance cassette (amplified with primers 82 and 83) and a 1 kb fragment homologous to the 3' downstream region of *mak-1* (generated with primers 1306 and 1307), resulting in the plasmid 738.

For the generation of the *Ptef-1-mak-2*$^{Q100A}$ strain, the fragments required for the construction of the gene knock-in cassette were amplified by PCR. A 1 kb genomic region positioned 2 kb upstream of the *mak-2* promoter (considering it to be the 1 kb region upstream of the coding read frame) was amplified with primers 1489 and 1490. The *Ptef-1-mak-2*$^{Q100A}$*-gfp* plasmid used in a previous study (Serrano et al., 2018) served as a template for the amplification of the *Ptef-1-mak-2*$^{Q100A}$ PCR fragment with primers 1488 and 1487. The resistance cassette used was *Hyg*$^{R}$, which was amplified with primers 82 and 83. Finally, the 1 kb genomic region downstream of the *mak-2* Stop-codon was amplified with primers 1489 and 1492. The four fragments were fused by yeast recombinational cloning generating the plasmid 846.. The plasmid 723 (*Ptef-1-dsRed-so*) was generated by cloning of the *so* ORF amplified with primers 1419 and 1420 and ligated

692 into the plasmid 722 (pMF334-Tef-dsRed) with enzymes AscI/XbaI. The resulting plasmid
693 was transformed into N1-03 generating the strain 843 (*his-3::Ptef-1-dsRed-so*). Yeast
694 recombinational cloning was performed as described elsewhere (Da et al., 2000).

695 *Strain generation*

696 All strains were either generated by transformation as described in early studies (Margolin
697 et al., 1997) or by crossing (Westergaard and Mitchell, 1947). When indicated, strains
698 were purchased to the Fungal Genetics Stock Center. A helpful list of protocols and media
699 description is available at their website (www.fgsc.net).

700 *Live-cell imaging*

701 Sample preparation was performed as previously described (Schürg et al., 2012). For
702 observation of hyphal fusion in *N. crassa*, 5 µl of a $10^7$-spore suspension were inoculated
703 on the side of a MM agar plate and incubated for 15 hours at 30ºC. The preparation of
704 the sample was performed in a similar way than for the spores. The microscope used and
705 the settings for software analyses were described in an early study (Serrano et al., 2018).
706 All fluorescence images shown in this study were processed by the widely used
707 commercial deconvolution software Huygens (by Scientific Volume Imaging), more
708 specifically the Huygens Essential version. Z-stacks (usually n=10) up to 100 nm of all
709 fluorescence images were captured and assembled as a single tiff file by using ImageJ
710 (image-stacks-image to stack). The composite images were processed through the
711 deconvolution software with the following parameters (40-100 iterations, 12 signal/noise
712 ratio and 0.01% of quality change thresh).

*Quantitative analyses*

Quantification of the cell fusion and germination rate was performed as described elsewhere (Fleissner et al., 2009; Schürg et al., 2012). For all cell fusion quantifications at least 100 spores were quantified per sample/condition, and at least three independent repetitions were studied.

*Chemical inhibition*

Three different chemicals were used for the corresponding experiments. Latrunculin A (10 µM), dissolved in water, was used to test the consequences of actin-polymerization inhibition, 1-NM-PP1 (40 µm) dissolved in DMSO was used to test the inhibition of the analog-sensitive kinases, and NSC23766 (100 µM/25 µM), dissolved in water, was used for specific inhibition of the Rho-GTPase RAC-1. As a control, either water or DMSO 1% was used. For all inhibitor experiments, fresh spores were harvested and incubated for 2 hours at 30ºC in MM plates. A 1 $cm^2$ piece was cut from the agar plate and inverted onto a coverslip. The chemical was added on the sample prior inversion onto the coverslip or on one side of the agar block.

*Statistics applied to the data*

All quantitative data were statistically analyzed by performing a two-tailed paired t-test using Excel. The P values were calculated for 0.001, 0.05 or 0.01, and indicated as ***, ** or * respectively. To analyze whether the variances were paired or unpaired, F-test analyses were performed.

**Achnowledgements**

We greatly acknowledge use of materials generated by the project ‘Functional analysis of a model filamentous fungus’, which was supported by a National Institutes of Health grant (PO1 GM068087).

## Funding

This work has been supported by funding from the Deutsche Forschungsgemeinschaft (FL706-2) and from the European Commission (PITN-GA-2013-607963).

## References

**Aguilar, P. S., Baylies, M. K., Fleissner, A., Helming, L., Inoue, N., Podbilewicz, B., Wang, H. and Wong, M.** (2013). Genetic basis of cell-cell fusion mechanisms. *Trends Genet* **29**, 427-37.

**Araujo-Palomares, C. L., Richthammer, C., Seiler, S. and Castro, L.** (2011). Functional Characterization and Cellular Dynamics of the CDC-42 - RAC - CDC-24 Module in *Neurospora crassa*. *PloS one* **6**.

**Berepiki, A., Lichius, A. and Read, N. D.** (2011). Actin Organization and Dynamics in Filamentous Fungi. *Nature reviews. Microbiology* **9**.

**Berepiki, A., Lichius, A., Shoji, J. Y., Tilsner, J. and Read, N. D.** (2010). F-actin dynamics in *Neurospora crassa*. *Eukaryot Cell* **9**, 547-57.

**Bishop, A. C., Ubersax, J. A., Petsch, D. T., Matheos, D. P., Gray, N. S., Blethrow, J., Shimizu, E., Tsien, J. Z., Schultz, P. G., Rose, M. D. et al.** (2000). A Chemical Switch for Inhibitor-Sensitive Alleles of Any Protein Kinase. *Nature* **407**.

**Correia, I., Alonso-Monge, R. and Pla, J.** (2010). MAPK Cell-Cycle Regulation in *Saccharomyces cerevisiae* and *Candida albicans*. *Future microbiology* **5**.

**Corvest, V., Bogliolo, S., Follette, P., Arkowitz, R. A. and Bassilana.** (2013). Spatiotemporal Regulation of Rho1 and Cdc42 Activity During *Candida albicans* Filamentous Growth. *Molecular microbiology* **89**.

**Coué, M., Brenner, S. L., Spector, I. and Korn, E.** (1987). Inhibition of Actin Polymerization by Latrunculin A. *FEBS letters* **213**.

**Da, B., Dawson, D. and Stearns, T.** (2000). Methods In Yeast Genetics: A Cold Spring Harbor Laboratory Course Manual.

**de Nobel, H., van Den Ende, H. and Klis, F. M.** (2000). Cell Wall Maintenance in Fungi. *Trends in microbiology* **8**.

**Dudin, O., Bendezú, F. O., Groux, R., Laroche, T., Seitz, A. and Martin.** (2015). A Formin-Nucleated Actin Aster Concentrates Cell Wall Hydrolases for Cell Fusion in Fission Yeast. *The Journal of cell biology* **208**.

**Dudin, O., Merlini, L., Bendezú, F. O., Groux, R., Vincenzetti, V. and Martin.** (2017). A Systematic Screen for Morphological Abnormalities During Fission Yeast Sexual Reproduction Identifies a Mechanism of Actin Aster Formation for Cell Fusion. *PLoS genetics* **13**.

**Fleissner, A., Leeder, A. C., Roca, M. G., Read, N. D. and Glass.** (2009). Oscillatory Recruitment of Signaling Proteins to Cell Tips Promotes Coordinated Behavior During Cell Fusion. *Proceedings of the National Academy of Sciences of the United States of America* **106**.

**Fleissner, A., Sarkar, S., Jacobson, D. J., Roca, M. G., Read, N. D. and Glass.** (2005). The So Locus Is Required for Vegetative Cell Fusion and Postfertilization Events in *Neurospora crassa*. *Eukaryotic cell* **4**.

**Fleißner, A. and Serrano, A.** (2016). 7 The Art of Networking: Vegetative Hyphal Fusion in Filamentous Ascomycete Fungi. In *Growth, Differentiation and Sexuality*, (ed. J. Wendland), pp. 133-153. Cham: Springer International Publishing.

**Fu, C., Ao, J., Dettmann, A., Seiler, S. and Free, S. J.** (2014). Characterization of the *Neurospora crassa* Cell Fusion Proteins, HAM-6, HAM-7, HAM-8, HAM-9, HAM-10, AMPH-1 and WHI-2. *PloS one* **9**.

**Fu, C., Priyadarshini, I., Amrita, H., Julia, A., Angela, S. and Stephen, J.** (2011). Identification and Characterization of Genes Required for Cell-to-Cell Fusion in *Neurospora crassa*.

**Goryachev, A. B., Lichius, A., Wright, G. D. and Read.** (2012). Excitable Behavior Can Explain the "Ping-Pong" Mode of Communication Between Cells Using the Same Chemoattractant. *BioEssays : news and reviews in molecular, cellular and developmental biology* **34**.

**Levin, D. E.** (2011). Regulation of Cell Wall Biogenesis in *Saccharomyces cerevisiae*: The Cell Wall Integrity Signaling Pathway. *Genetics* **189**.

**Lichius, A., Goryachev, A. B., Fricker, M. D., Obara, B., Castro-Longoria, E. and Read.** (2014). CDC-42 and RAC-1 Regulate Opposite Chemotropisms in *Neurospora crassa*. *Journal of cell science* **127**.

**Maddi, A., Dettman, A., Fu, C., Seiler, S. and Free, S. J.** (2012). WSC-1 and HAM-7 Are MAK-1 MAP Kinase Pathway Sensors Required for Cell Wall Integrity and Hyphal Fusion in *Neurospora crassa*. *PloS one* **7**.

**Maerz, S., Ziv, C., Vogt, N., Helmstaedt, K., Cohen, N., Gorovits, R., Yarden, O. and Seiler, S.** (2008). The Nuclear Dbf2-related Kinase COT1 and the Mitogen-Activated Protein Kinases MAK1 and MAK2 Genetically Interact to Regulate Filamentous Growth, Hyphal Fusion and Sexual Development in *Neurospora crassa*. *Genetics* **179**.

**Makushok, T., Alves, P., Huisman, S. M., Kijowski, A. R. and Brunner, D.** (2016). Sterol-Rich Membrane Domains Define Fission Yeast Cell Polarity. *Cell* **165**.

**Margolin, B. S., M. Freitag and Selker., E. U.** (1997). Improved plasmids for gene targeting at the his-3 locus of Neurospora crassa by electroporation,. *Fungal Genetics Reports* **44**.

**Martin, S. G. and Arkowitz, R. A.** (2014). Cell polarization in budding and fission yeasts. *FEMS Microbiol Rev* **38**, 228-53.

**Matheos, D., Metodiev, M., Muller, E., Stone, D. and Rose, M. D.** (2004). Pheromone-induced Polarization Is Dependent on the Fus3p MAPK Acting Through the Formin Bni1p. *The Journal of cell biology* **165**.

**Ninomiya, Y., Suzuki, K., Ishii, C. and Inoue.** (2004). Highly Efficient Gene Replacements in *Neurospora* Strains Deficient for Nonhomologous End-Joining. *Proceedings of the National Academy of Sciences of the United States of America* **101**.

**Pandey, A., Roca, M. G., Read, N. D. and Glass.** (2004). Role of a Mitogen-Activated Protein Kinase Pathway During Conidial Germination and Hyphal Fusion in Neurospora Crassa. *Eukaryotic cell* **3**.

**Park, G., Pan, S. and Borkovich, K. A.** (2008). Mitogen-activated Protein Kinase Cascade Required for Regulation of Development and Secondary Metabolism in *Neurospora crassa*. *Eukaryotic cell* **7**.

**Qi, M. and Elion, E.** (2005). Formin-induced Actin Cables Are Required for Polarized Recruitment of the Ste5 Scaffold and High Level Activation of MAPK Fus3. *Journal of cell science* **118**.

**Riedl, J., Crevenna, A. H., Kessenbrock, K., Yu, J. H., Neukirchen, D., Bista, M., Bradke, F., Jenne, D., Holak, T. A., Werb, Z. et al.** (2008). Lifeact: A Versatile Marker to Visualize F-actin. *Nature methods* **5**.

**Roca, M. G., Kuo, H. C., Lichius, A., Freitag, M. and Read, N.** (2010). Nuclear Dynamics, Mitosis, and the Cytoskeleton During the Early Stages of Colony Initiation in *Neurospora crassa*. *Eukaryotic cell* **9**.

**Schürg, T., Brandt, U., Adis, C. and Fleissner, A.** (2012). The Saccharomyces Cerevisiae BEM1 Homologue in *Neurospora crassa* Promotes Co-Ordinated Cell Behaviour Resulting in Cell Fusion. *Molecular microbiology* **86**.

**Serrano, A., Hammadeh, H. H., Herzog, S., Illgen, J., Schumann, M. R., Weichert, M. and Fleiβner.** (2017). The Dynamics of Signal Complex Formation Mediating Germling Fusion in *Neurospora crassa*. *Fungal genetics and biology : FG & B* **101**.

**Serrano, A., Illgen, J., Brandt, U., Thieme, N., Letz, A., Lichius, A., Read, N. D. and Fleissner, A.** (2018). Spatio-temporal MAPK dynamics mediate cell behavior coordination during fungal somatic cell fusion. *J Cell Sci* **131**.

**Vogel, J. H.** (1956). A convenient growth medium for *Neurospora* (medium N). *Microbial Genetics Bulletin* **13**, 42-43.

**Vogt, N. and Seiler, S.** (2008). The RHO1-specific GTPase-activating Protein LRG1 Regulates Polar Tip Growth in Parallel to Ndr Kinase Signaling in *Neurospora*. *Molecular biology of the cell* **19**.

**Weichert, M., Lichius, A., Priegnitz, B. E., Brandt, U., Gottschalk, J., Nawrath, T., Groenhagen, U., Read, N. D., Schulz, S. and Fleissner, A.** (2016). Accumulation of specific sterol precursors targets a MAP kinase cascade mediating cell-cell recognition and fusion. *Proc Natl Acad Sci U S A* **113**, 11877-11882.

**Westergaard, M. and Mitchell, H. K.** (1947). *Neurospora* V. A Synthetic Medium Favoring Sexual Reproduction. *Am. J. Bot.* **34**, 573-577.

**Yoshimi, A., Miyazawa, K. and Abe, K.** (2016). Cell Wall Structure and Biogenesis in *Aspergillus* Species. *Bioscience, biotechnology, and biochemistry* **80**.

## Figures

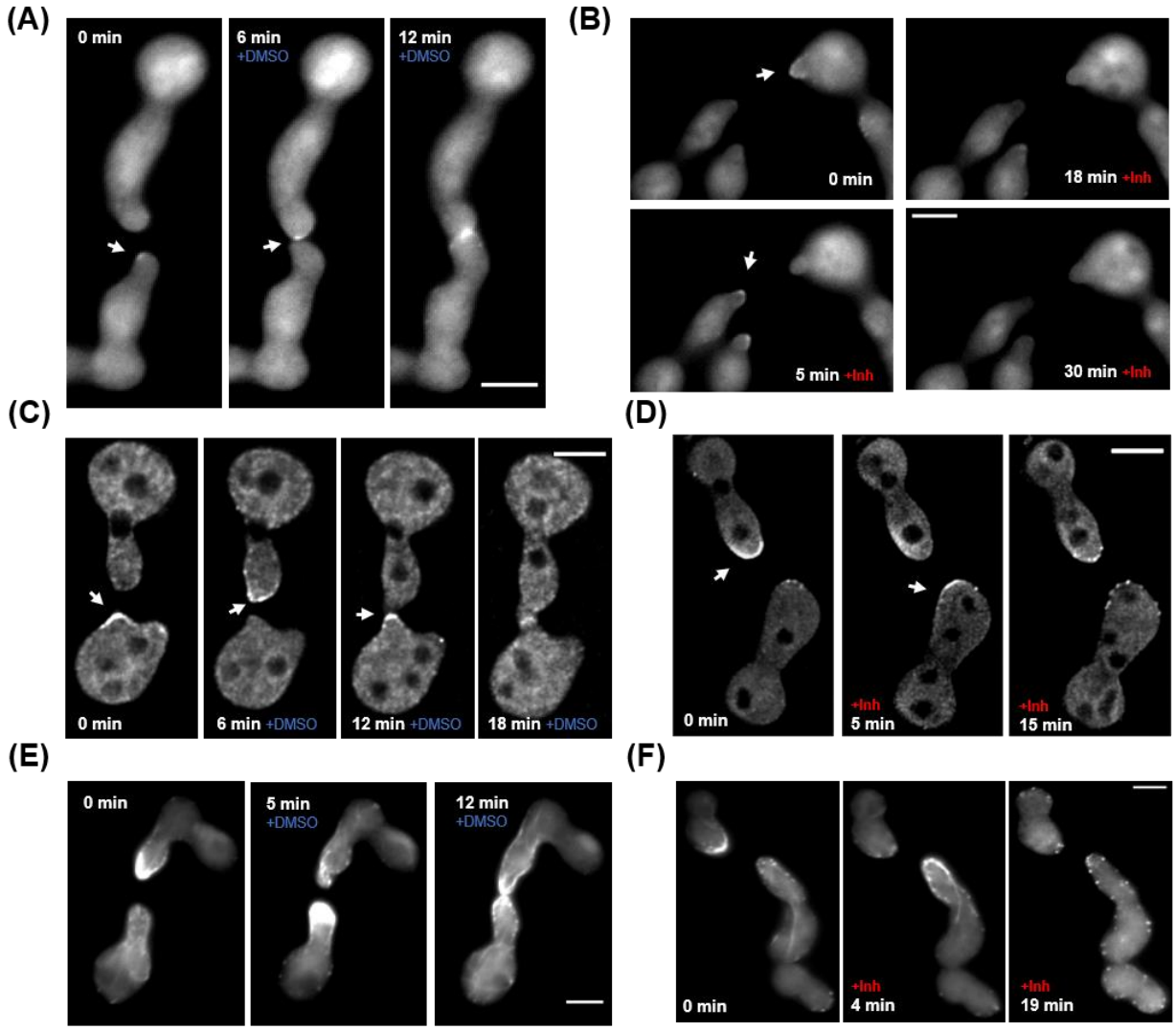


**Figure 1. Activity inhibition of MAK-1 disrupts the oscillatory localization of MAK-2/SO and the formation of the fusion actin aster at the cell tips**. **(A)** Oscillatory localization of MAK-2-GFP when DMSO (1%) is added in the strain 865 (*mak-1::mak-1$^{E104G}$-hph*; *his-3::Ptef-1-mak-2-gfp*). **(B)** Addition of 1-NM-PP1 (40 µM) disrupts the oscillatory dynamic localization of MAK-2 in strain 865. **(C)** Oscillatory dynamic localization of SO when DMSO (1%) is added in the strain 874 (*mak-1::mak-1$^{E104G}$-hph*; *his-3::Ptef-1-so-gfp*). **(D)** Addition of 1-NM-PP1 (40 µM) disrupts the oscillatory dynamic localization of SO in strain 874. **(E)** Localization of actin (through lifeact-gfp) when DMSO (1%) is added in the strain 869 (*mak-1::mak-1$^{E104G}$-hph*; *his-3::Ptef-1-lifeact-gfp*) **(F)** Addition of 1-NM-PP1 (40 µM) disrupts the localization of actin at the cell tips of the interacting cells, in strain 869. All observations were made multiple times (n≥15). Scale bars 5 µm.

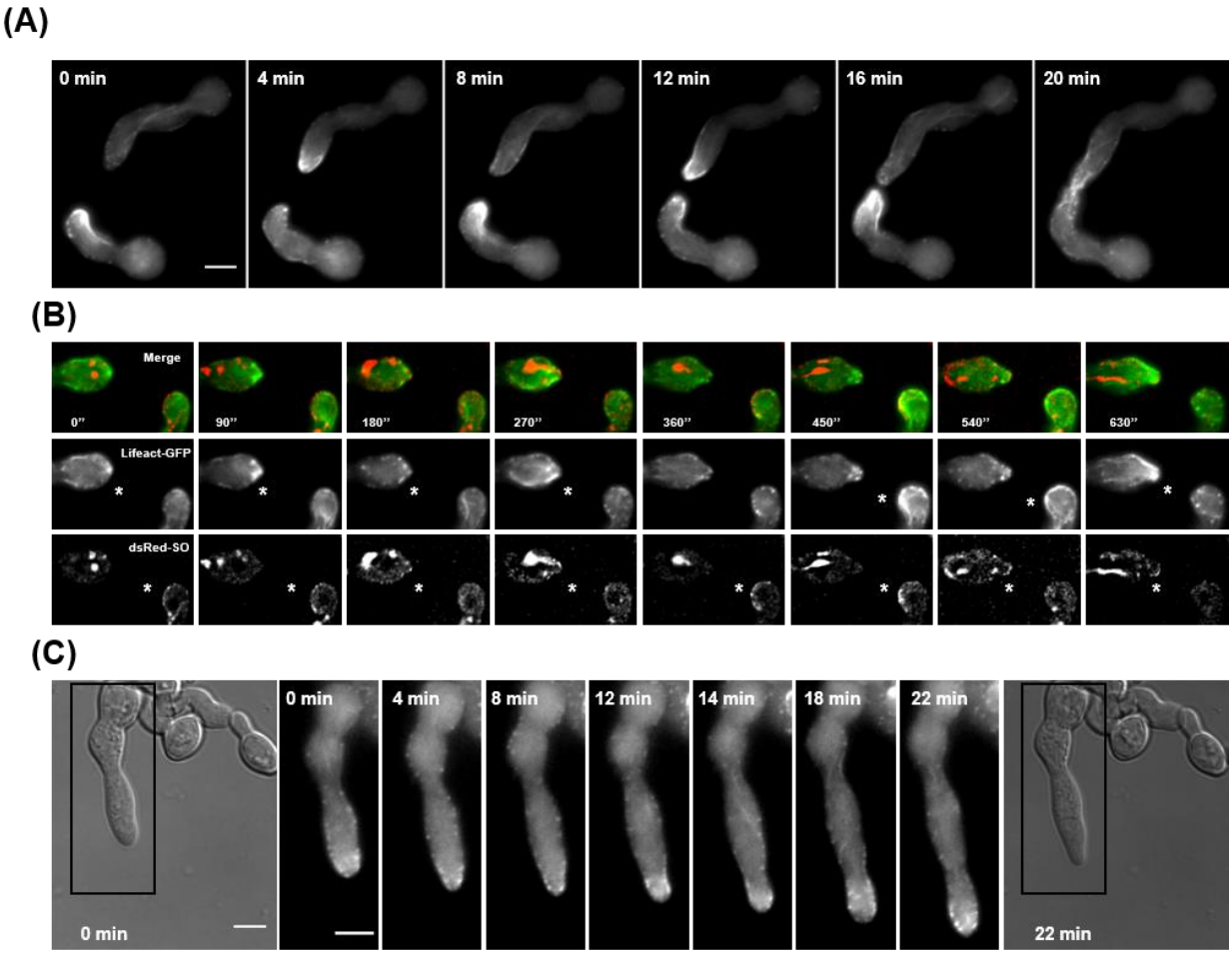


**Figure 2. Actin focalize to the tips of the interactings cells in an oscillatory manner. (A)** Oscillatory dynamic localization of actin fusion aster at the cell tips of the interacting cells in strain 754 (*his-3::Ptef-1-lifeact-gfp*). **(B)** Actin (Lifeact-GFP) co-localization with dsRed-SO during the interaction of fusing cells in the heterokaryon created with strains 754 and N1-30. Similar observation were made three times. **(C)** Actin localization in non-interacting cell vegetative growth, strain 754. Similar observations for A and C were made multiple times (n=10). Scale bars 5 µm

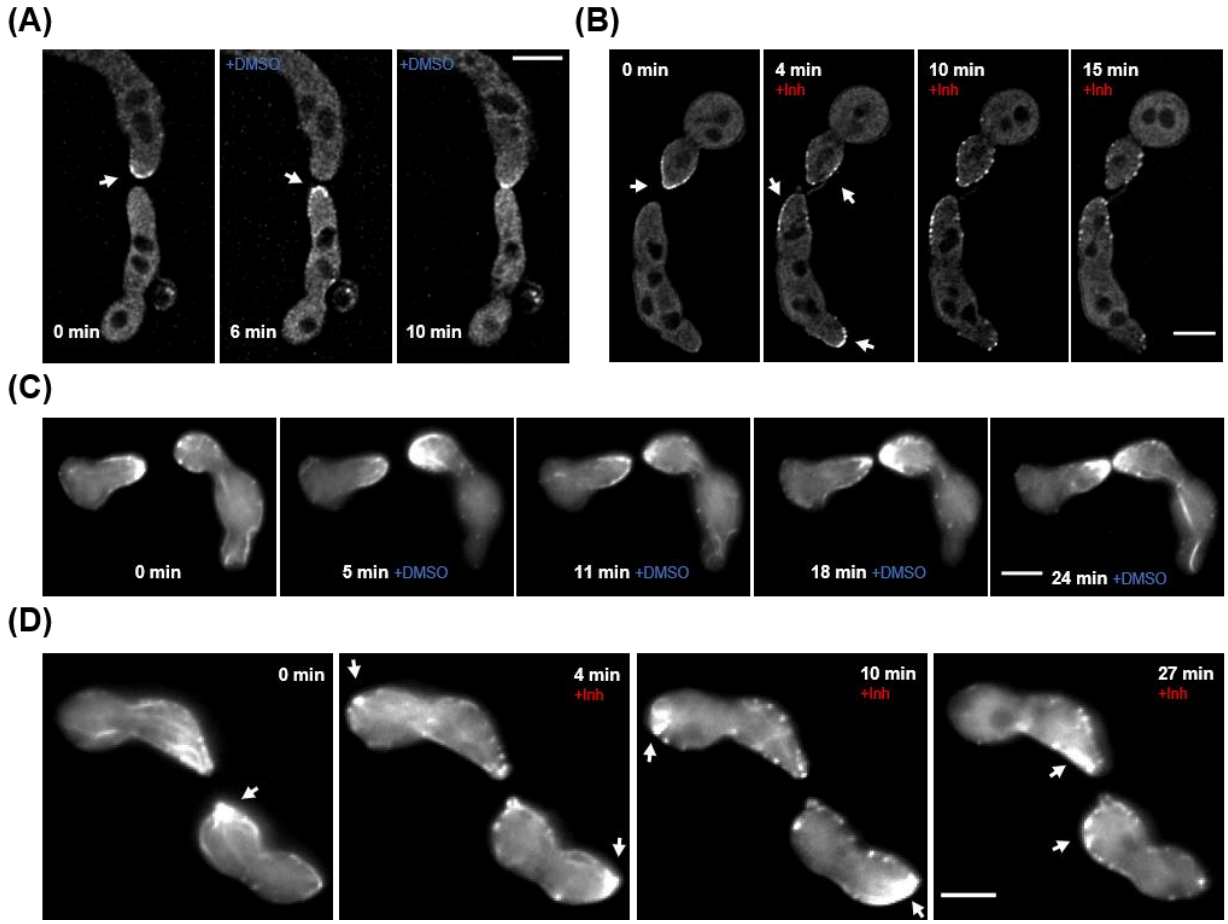


**Figure 3. Activity inhibition of MAK-2 disrupts the SO dynamic localization and mislocalizes actin around the cell membrane**. **(A)** Oscillatory localization of SO-GFP when DMSO (1%) is added in the strain 912 (*Pmak-2-mak-2::Ptef-1-mak-2*$^{Q100A}$*-hph*; *his-3::Ptef-1-so-gfp*). **(B)** Addition of 1-NM-PP1 (40 µM) disrupts the oscillatory dynamic localization of SO in strain 912. **(C)** Oscillatory localization of actin when DMSO (1%) is added in the strain 915 (*Pmak-2-mak-2::Ptef-1-mak-2*$^{Q100A}$*-hph*; *his-3::Ptef-1-lifeact-gfp*). **(D)** Addition of 1-NM-PP1 (40 µM) disrupts the oscillatory dynamic localization of actin in strain 915. All observations were made multiple times (n≥10). Scale bars 5 µm.

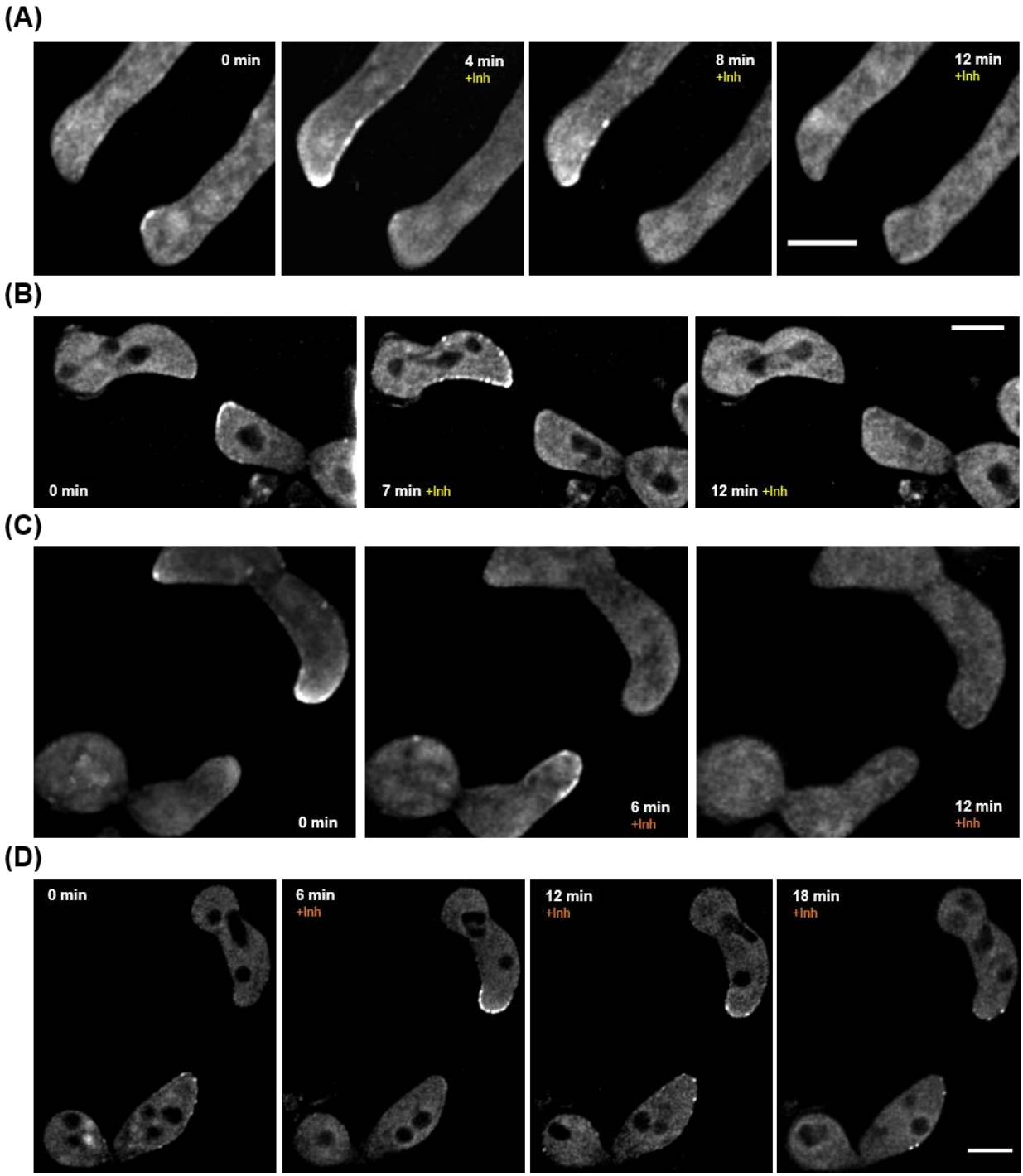


**Figure 4. Inhibition of actin assembly disrupts the MAK-2/SO dynamic localization. (A)** Inhibition of actin with latrunculin A (10 µM) disrupts the localization of MAK-2 in strain 865 (*mak-1::mak-1$^{E104G}$-hph*; *his-3::Ptef-1-mak-2-gfp*) **(B)** Inhibition of actin with latrunculin A (10 µM) disrupts the localization of SO in strain 874 (*mak-1::mak-1$^{E104G}$-hph*; *his-3::Ptef-1-so-gfp*). **(C)** Inhibition of RAC-1 with NSC23766 (100 µM) disrupts the localization of MAK-2 in strain 865 (*mak-1::mak-1$^{E104G}$-hph*; *his-3::Ptef-1-mak-2-gfp*) (Next page)

**(D)** Inhibition of RAC-1 with NSC23766 (100 µM) disrupts the localization of SO in strain 874 (*mak-1::mak-1*$^{E104G}$*-hph*; *his-3::Ptef-1-so-gfp*). All observations were made multiple times (n≥10). Scale bars 5 µm.

*(Figure 5 in next page)*

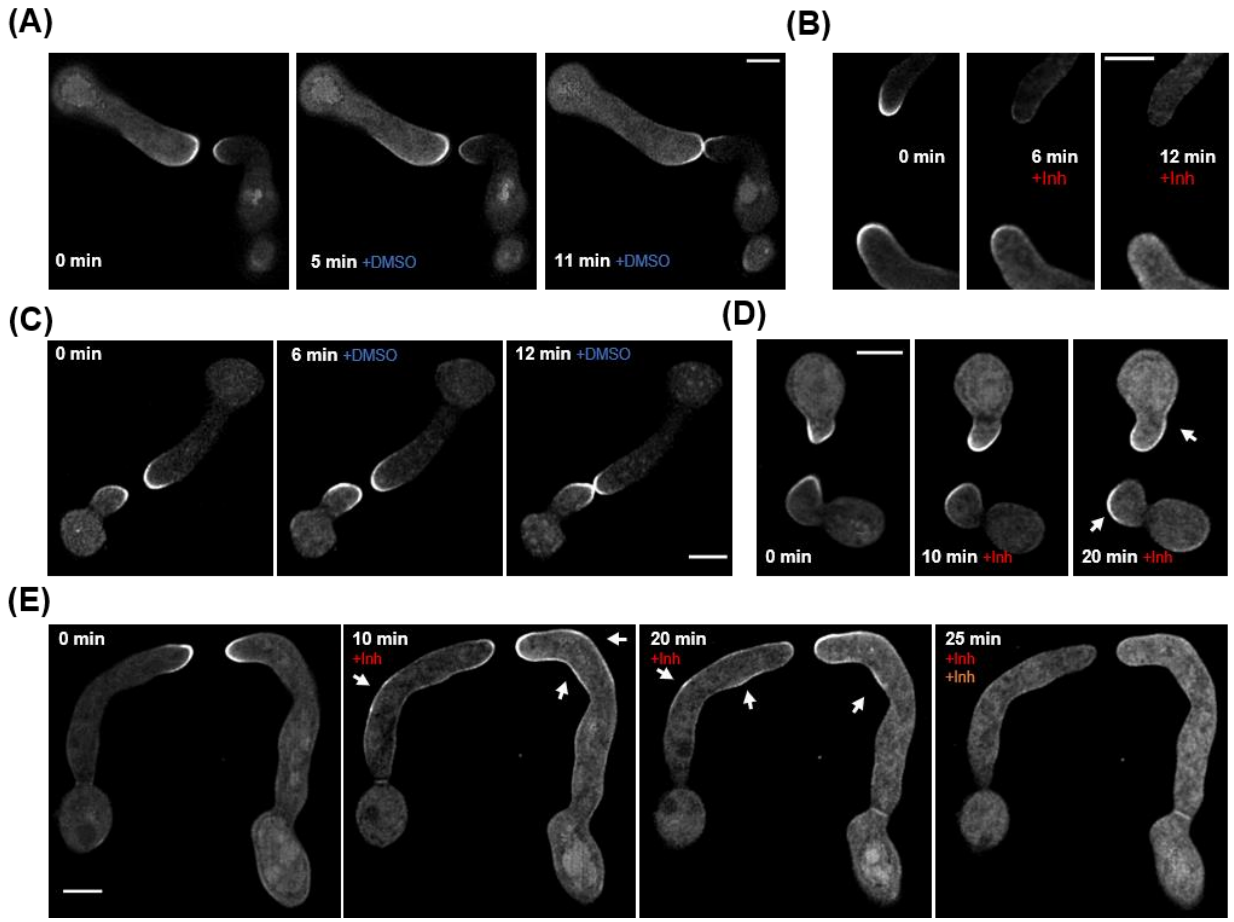


**Figure 5. Activity inhibition of MAK-1 results in RAC-1 inactivation while MAK-2 inhibition results in RAC-1 mislocalization. (A)** Localization of activated RAC-1/CDC-42 in both cell tips through the CRIB reporter (CRIB-GFP) during cell fusion when DMSO (1%) is added in strain 943 (*mak-1::mak-1*$^{E104G}$*-hph; Pal1-crib*$^{cla-4}$*-bar*). **(B)** Disruption in CRIB-GFP localization when 1-NM-PP1 (40 µM) is added in strain 943. **(C)** Localization of activated RAC-1/CDC-42 in both cell tips through the CRIB reporter (CRIB-GFP) during cell fusion when DMSO (1%) is added in strain 949 (*Pmak-2-mak-2::Ptef-1-mak-2*$^{Q100A}$*-hph;Pal1-crib*$^{cla-4}$*-bar*). **(D)** Mislocalization of CRIB-GFP localization when 1-NM-PP1 (40 µM) is added in strain 949. **(E)** Localization of the CRIB-GFP when 1-NM-PP1 (40 µM) is added in strain 949, followed by inhibition of RAC-1 with NSC23766 (100 µM). Comparable observations were made multiple times (n≥10). Scale bars 5 µm.

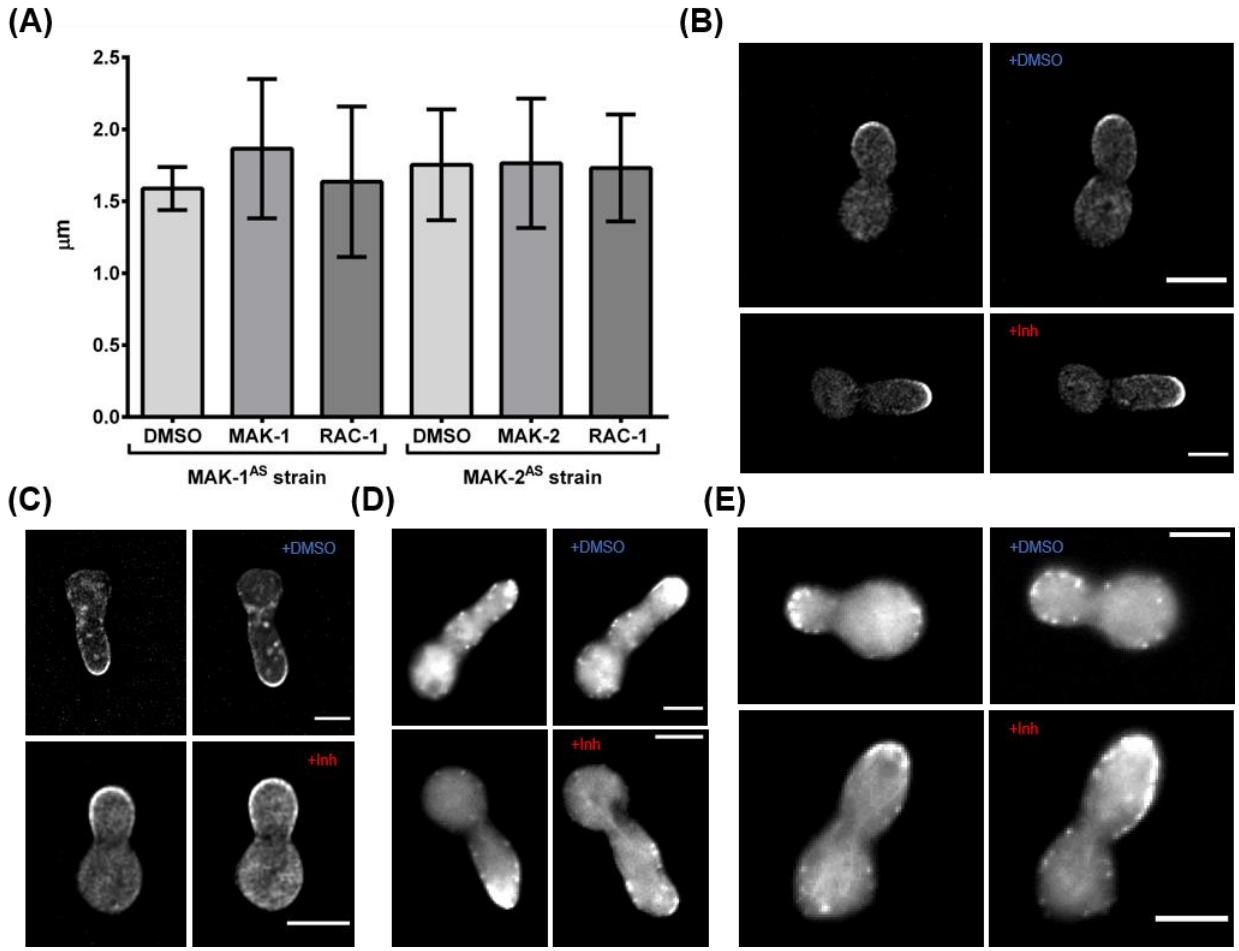


**Figure 6. Inhibition of either MAK-1 or RAC-1 does not affect actin localization in vegetative growth. (A)** Growth quantification in cells treated as control (DMSO 1%), 1-NM-PP1 40 µM (MAK-1/MAK-2 inhibition) and NSC23766 100 µM (RAC-1 inhibition). No significant differences are observed between all tests (n≥25). **(B)** Upper panel: localization of the CRIB reporter in strain 943 (*mak-1::mak-1*$^{E104G}$*-hph; Pal1-crib*$^{cla-4}$*-bar*) in cells treated with DMSO (1%) before and 30 minutes after addition. Bottom panel: localization of the CRIB reporter in strain 943 in cells treated with 1-NM-PP1 (40 µM) before and 30 minutes after addition. **(C)** Upper panel: localization of the CRIB reporter in strain 949 (*Pmak-2-mak-2::Ptef-1-mak-2*$^{Q100A}$*-hph;Pal1-crib*$^{cla-4}$*-bar*) in cells treated with DMSO (1%) before and 30 minutes after addition. Bottom panel: localization of the CRIB reporter in strain 949 in cells treated with 1-NM-PP1 (40 µM) before and 30 minutes after addition. **(D)** Upper panel: localization of actin (Lifeact-GFP) in strain 869 (*mak-1::mak-1*$^{E104G}$*-hph*; *his-3::Ptef-1-lifeact-gfp*) in cells treated with DMSO (1%) before and 30 minutes after addition. Bottom panel: localization of actin (Lifeact-GFP) in strain 869 in cells treated with 1-NM-PP1 (40 µM) before and 30 minutes after addition. **(E)** Upper panel: localization of actin (Lifeact-GFP) in strain 915 (*Pmak-2-mak-2::Ptef-1-mak-2*$^{Q100A}$*-hph*; *his-3::Ptef-1-lifeact-gfp*) in cells treated with DMSO (1%) before and 30 minutes after addition. Bottom panel: localization of actin (Lifeact-GFP) in strain 915 in cells treated with 1-NM-PP1 (40 µM) before and 30 minutes after addition. Similar observations were made multiple times (n≥5). Scale bars 5 µm.

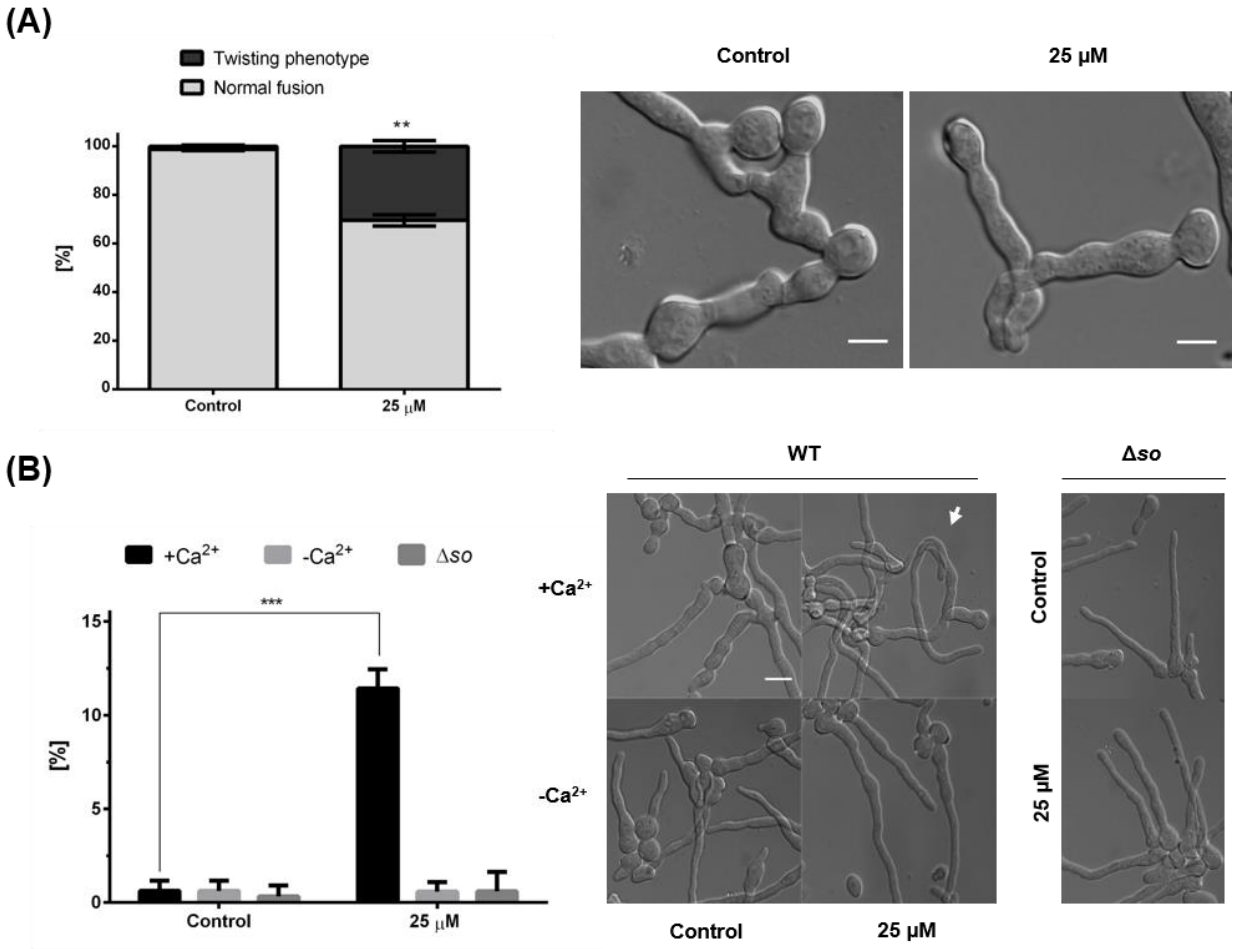


**Figure 7. RAC-1 and MAK-1 acts within the same pathway. (A)** Quantification of the observation of twisting cell fusion growth during partial inhibition of RAC-1. Control ($H_2O$) and 25 µM (NSC23766). Significant differences were observed between the number of twisting growth observations made in the presence of the inhibitor compare to the control (n≥100) **(B)** Quantification of polarity growth defects when RAC-1 is partially inhibited during cell fusion. Control ($H_2O$) and 25 µM (NSC23766), in media with $Ca^{2+}$ or without. Significant differences were observed between the partial inhibition and the control only in the present of $Ca^{2+}$.

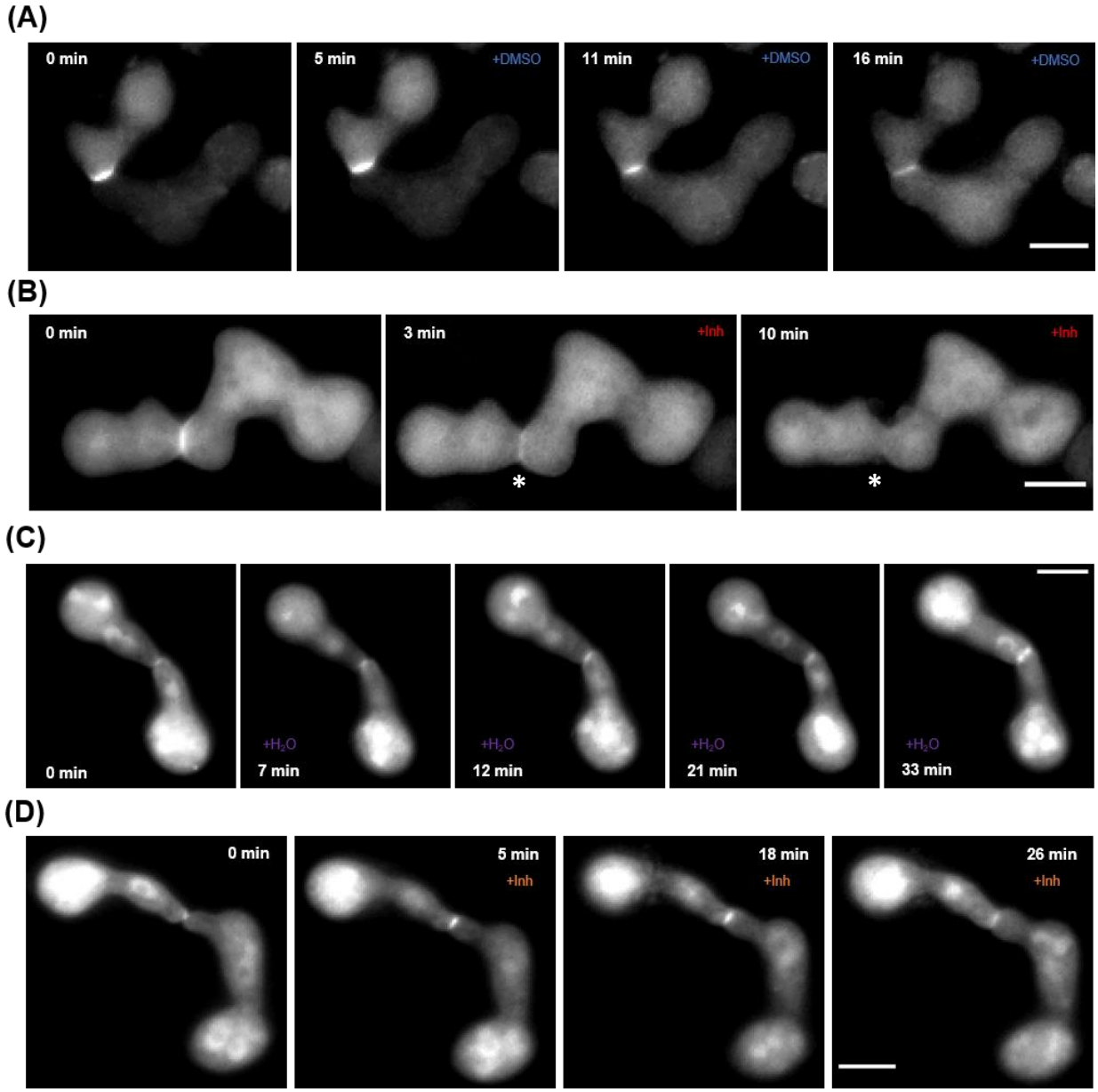


**Figure 8. MAK-1 is upstream of RAC-1. (A)** Localization of the CRIB-GFP during cell fusion when cells establish physical contact in strain 943 (*mak-1::mak-1$^{E104G}$-hph; Pal1-crib$^{cla-4}$-bar*) in cells treated with DMSO (1%). **(B)** Localization of the CRIB-GFP in strain 943 when MAK-1 is fully inhibited (with 1-NM-PP-1, 100 µM) in cells that just established physical contact. (*) to point the cell fusion event and signal dissapearence. **(C)** Localization of MAK-1-GFP in strain MW513 (*mak-1::hph; his-3::Pccg-1-mak-1-gfp*) with $H_2O$. **(D)** Localization of MAK-1-GFP when RAC-1 is fully inhibited with NSC23766 (100 µM). Similar observations were made multiple times (n=10) Scale bars 5 µm.